Cell Tissue Res (2009) 337:491–511
DOI 10.1007/s00441-009-0831-9

REGULAR ARTICLE

Constancy and variability of identified glomeruli in antennal lobes: computational approach in *Spodoptera littoralis*

Louise Couton · Sebastian Minoli · Kiên Kiêu · Sylvia Anton · Jean-Pierre Rospars

Received: 19 December 2008 / Accepted: 19 June 2009 / Published online: 1 August 2009

Abstract The primary olfactory centres share striking similarities across the animal kingdom. The most conspicuous is their subdivision into glomeruli, which are spherical neuropil masses in which synaptic contacts between sensory and central neurons occur. Glomeruli have both an anatomical identity (being invariant in location, size and shape) and a functional identity (each glomerulus receiving afferents from olfactory receptor neurons that express the same olfactory receptor). Identified glomeruli offer a favourable system for analysing quantitatively the constancy and variability of the neuronal circuits, an important issue for understanding their function, development and evolution. The noctuid moth *Spodoptera littoralis* with its well-studied pheromone communication system has become a model species for olfaction research. We analyse here its glomerular organisation based on ethyl-gallate-stained and synapsin-stained preparations. Although we have confirmed that the majority of glomeruli can be individually identified in various antennal lobes, we have recognised several types of biological variability. Some glomeruli are absent, possibly indicating the lack of the corresponding receptor neuron type or its misrouting during development. The antennal lobes vary in global shape and, consequently, the spatial location of the glomerular changes. Although they do not prevent glomerulus identification when quantitative analysis methods are used, these variations place limits on the straightforward identification of glomeruli in functional studies, e.g. calcium-imaging or single-cell staining, when using conventional three-dimensional maps of individual antennal lobes.

Keywords Olfaction · Computational neuroanatomy · Three-dimensional reconstruction · Identified glomeruli · Moth, *Spodoptera littoralis* (Insecta)

This work was supported by research grants from INRA (Projet Jeune Equipe and Projet S.P.E.) to S.A. and J.P.R. and from ANR-BBSRC 07 BSYS 006 (Pherosys) to J.P.R. and S.A. and by a PhD grant from INRA Departments M.I.A. and S.P.E. to L.C.

Electronic supplementary material The online version of this article (doi:10.1007/s00441-009-0831-9) contains supplementary material, which is available to authorised users.

L. Couton · S. Minoli · S. Anton · J.-P. Rospars
INRA, UMR 1272 Physiologie de l'Insecte,
78000 Versailles, France

L. Couton · K. Kiêu · J.-P. Rospars
INRA, UR 341, Mathématiques et Informatique Appliquées,
78350 Jouy-en-Josas, France

J.-P. Rospars (✉)
INRA, Centre de Versailles, UMR1272,
Route de St. Cyr,
78000 Versailles, France
e-mail: rospars@versailles.inra.fr

Introduction

The sense of smell is of critical importance in most animal species and is used in many different contexts including the recognition and selection of food items, communication with mating partners and identification of predators. The primary olfactory centres, namely the antennal lobe (AL) in insects and the olfactory bulb in vertebrates, share many common features throughout the animal kingdom (for reviews, see Hildebrand and Shepherd 1997; Strausfeld and Hildebrand 1999), especially their subdivision into spherical substructures called the glomeruli.

In insects, the glomeruli house all synaptic connections between the olfactory receptor neurons (ORNs), which

come from antennal olfactory sensilla, and higher order neurons (Distler and Boeckh 1996, 1997; Sun et al. 1997). The latter neurons belong to three main categories: local neurons (LNs), projection neurons (PNs) and centrifugal neurons. LNs are restricted to the AL and connect glomeruli to one another, whereas PNs connect the glomeruli to higher centres, the mushroom bodies and the lateral protocerebrum (for reviews, see Anton and Homberg 1999; Hansson and Anton 2000). A noteworthy feature of insect glomeruli is that they have been shown to be invariant, each glomerulus having the same shape, size and location across individuals of the same species, sex and developmental stage (Chambille et al. 1980; for a review, see Rospars 1988; see also references in AL atlases below). This invariance results from several properties of the neuronal processes arborising within the glomeruli. First, the axon of each ORN terminates in a single glomerulus in most insects (for reviews, see Anton and Homberg 1999; Hansson and Anton 2000). Second, all ORNs projecting to a given glomerulus bear the same type of olfactory receptor protein (Gao et al. 2000; Vosshall et al. 2000). Third, the dendritic arborisations of many PNs are also restricted to a single glomerulus (e.g. Wilson et al. 2004; Reisenman et al. 2005). Thus, each glomerulus possesses a "structural identity".

This structural identity corresponds to a functional identity. The main function of the glomerular array is to analyse an odour, usually composed of a complex mixture of various odorants, into a set of "primary odour qualities", each glomerulus representing one primary odour (Heisenberg 2003). According to this view, any odour is coded by the activation of a specific set of glomeruli (Rospars 1983). This pattern has been revealed by calcium-imaging (e.g. Sachse and Galizia 2002). However, other functions of glomerular compartmentalisation have been suggested. Within each glomerulus, a large number of ORNs (between 20 and 2000) converge onto a much smaller number of PNs (two to three; for a review, see Anton and Homberg 1999). This convergence implies a large decrease of the redundancy and imprecision of the olfactory message carried by ORNs. It readily explains why PNs have a sensory threshold 10- to 100-fold lower than ORNs (Boeckh and Boeckh 1979; for a review, see Hansson and Christensen 1999). Other suggested functions can be attributed to the glomeruli as spatial units of the neuronal circuitry, such as the relative stability of glomerular activation patterns whatever the odour concentration (e.g. Zube et al. 2008) and the enhancement of contrast with respect to the ORN activation pattern (Sachse and Galizia 2002; Silbering and Galizia 2007; Reisenman et al. 2008). All these functions involve LNs (Wilson and Laurent 2005; Linster et al. 2005).

The number of glomeruli varies from around 50 in mosquitoes (Ignell et al. 2005) up to a thousand in *Vespa crabro* (Hanström 1928) and in the locust (Ernst et al. 1977), the locust representing an exceptional case with its multiglomerular ORNs and PNs (Ignell et al. 2001; Anton et al. 2002). The most common numbers in insects are in the range of 50 to 200 (Anton and Homberg 1999; Rospars 1988; Schachtner et al. 2005), giving an approximate idea of the number of expressed olfactory receptors and of physiological classes of ORNs (Vosshall et al. 2000). In *Drosophila*, almost complete maps of olfactory receptor expression in ORNs and ORN projection in glomeruli have been constructed that confirm the general validity of the "one ORN-one receptor" and "one glomerulus-one receptor" principles (Couto et al. 2005; Fishilevich and Vosshall 2005; Ray et al. 2007). The invariance of the glomerular array has been investigated in various insect orders and has led to the establishment of AL atlases, e.g. in Lepidoptera (Berg et al. 2002; Greiner et al. 2004; Kazawa et al. 2009; Masante-Roca et al. 2005; Rospars 1983; Rospars and Hildebrand 1992; Sadek et al. 2002; Skiri et al. 2005), Diptera (Ignell et al. 2005; Ghaninia et al. 2007; Laissue et al. 1999; Pinto et al. 1988; Stocker et al. 1990), Blattaria (Rospars and Chambille 1986) and Hymenoptera (Arnold et al. 1985; Flanagan and Mercer 1989; Galizia et al. 1999).

The present work is devoted to the AL of the noctuid moth *Spodopera littoralis* and focuses on the constancy and variability of their glomerular organisation. These two linked issues are becoming increasingly important for the standardisation of anatomical maps and, more generally, for the analysis of neural tissues in terms of single neurons and well-defined neuronal networks from a structural, functional, developmental and evolutionary perspective (Rein et al. 2002; Kurylas et al. 2008). Glomeruli offer a particularly favourable case to investigate this general problem in neurobiology because they constitute an intermediate level of organisation, which magnifies the underlying neuronal connections and has the potential to express their regularities and irregularities, and also because they are amenable to a rigorous quantitative description. By means of standard methods in current computational neuroanatomy, the ALs of *S. littoralis* have been segmented and three-dimensionally reconstructed. These reconstructions have been compared visually in order to identify the corresponding glomeruli in all ALs and computational methods have been applied aimed at quantifying their position and size. With these data sets, the question of the constancy and variability of the AL organisation can be addressed. More specifically, we have aimed at distinguishing the different kinds of glomerular variability, mostly of biological origin, such as global deformations of the AL and random local changes in glomerular position. These observations at the neuropil level raise questions concerning the underlying variations of neuron connections and information processing in the AL neural network.

Materials and methods

Insects

Spodoptera littoralis were obtained from a laboratory colony kept at the INRA research centre in Versailles. Insects were reared on an artificial diet, under an 8/14 h dark/light cycle, at 20°C or 23°C and 70% relative humidity. Pupae were sexed and, from this pupal stage onwards, each sex was reared in a separate room. Adult eclosion was checked at the end of each scotophase and newly emerged males were used to profit from optimal tissue permeability. Moths were anaesthetised on ice prior to dissection of the brain.

Histology

Synapsin immunostaining A number of staining techniques for confocal observations were tested, such as autofluorescence (with glutaraldehyde fixation) or double phalloidin-synapsin immunostaining, with or without a dehydration and rehydration step. The best resolution of glomeruli was obtained with synapsin staining, as follows. The dissected brains were first fixed in a 4% paraformaldehyde solution in phosphate-buffered saline (PBS; 27.4 mM NaCl, 0.54 mM KCl, 1.6 mM Na_2HPO_4, 0.28 mM KH_2PO_4, pH 6.9). To make membranes more permeable, the brains were incubated overnight in 4% Triton X, rinsed and subsequently dehydrated and rehydrated in an alcohol series. The tissues were then incubated for 5 days in the primary antibody raised in mouse (DSHB, IA, USA; Klagges et al. 1996), 4 µl anti-synapsin being diluted with 96 µl PBS containing 0.25% Triton X (PBST) at 4°C, rinsed in PBST and incubated for 3 days in the secondary antibody (Invitrogen, Abingdon, UK) at a dilution of 1.5 µl anti-mouse-Alexa 546 to 250 µl PBST at 4°C. After being rinsed in PBST, brains were finally cleared and mounted in Vectashield (Vector laboratories, Burlingame, Calif., USA) and kept in the dark until scanned. A confocal microscope (SP2 AOBS, Leica, Heidelberg, Germany) was used to create three stacks of images for each brain: a detailed view of each AL and an overview of the brain. The microscope was equipped with a HC PL APO CS 10.0× 0.40NA UV air objective. Brains were scanned at a resolution of 1024×1024 pixels, with a step size of 2 µm in detailed views and 3 µm in overviews. Most preparations were scanned in parafrontal orientation and some in parahorizontal orientation. From more than 50 brains, three well-stained brains with a good parafrontal orientation, i.e. with the focal plane nearly perpendicular to the sagittal plane, were chosen for reconstruction and analysis. Finally, only the two best synapsin preparations (slm4 and slm5) were kept for full quantitative analyses. However, even in these two preparations, the glomeruli in the deepest optical sections proved difficult to resolve. Another limitation was an incorrect subcylindric (instead of subspherical) shape of the glomeruli in reconstructions. The orientation of the long axis of the cylinders was perpendicular to the sectioning plane suggesting that this artefactual effect resulted from an insufficient resolution of the fluorescence in nearby optical sections. In order to resolve the residual uncertainties in confocal data, we resorted to classical histology.

Ethyl gallate staining Osmium-ethyl gallate staining of dissected brains was carried out according to Leise and Mulloney (1986). The brains were first immersed in 2% glutaraldehyde and 1% paraformaldehyde in cacodylate buffer containing 1.3 g sucrose/100 ml buffer overnight at room temperature on a rotator. After a brief wash in buffer, they were incubated overnight in darkness at 4°C in 1% osmium tetroxide on a rotator. The tissues were then washed in buffer at 4°C, transferred to a supersaturated ethyl gallate solution overnight at 4°C in the dark, washed again in buffer and dehydrated in an ascending series of ethanol and propylene oxide. The brains were then embedded in Fluka Durcupan. Sections were cut at 5 µm with a glass knife on a microtome (RM2055, Leica Jung) and photographed on an Olympus BX50 microscope with either a UPlan FI 10× 0.3 (brain overviews) or a Plan N 20× 0.4 objective (detailed AL views). Ten brains were stained with ethyl gallate and physically sectioned. Three well-stained and well-oriented ethyl gallate preparations were fully reconstructed, based on parasagittal (slm1), parafrontal (slm2) and parahorizontal (slm3) sections.

Segmentation and three-dimensional reconstruction

For stacked images acquired on the confocal microscope, we proceeded as follows. First, the detailed confocal image stack of each AL was manually segmented, the outlines of the AL and of all visible glomeruli being drawn on each optical section. Within one AL, outlines belonging to the same glomerulus were given a provisional number. The refractive index mismatch between the air and the mounting medium causes a shortening in the axial dimension of the stack; this was corrected by applying a factor of 1.6 to the apparent thickness of the optical sections (Bucher et al. 2000; Anton and Rospars 2004). Based on the coordinates of the outlines, three-dimensional surface reconstructions of glomeruli were then computed. Depending on the preparations, segmentation and reconstruction were achieved by using Amira (Mercury Computer Systems SAS, Mérignac, France) or a custom-made program developed in the Matlab language (The MathWorks, Natick, USA). The latter module

was based on Nuages software (Boissonnat and Geiger 1993), a C program available in source code (http://www-sop.inria.fr/prisme/prisme_eng.html).

The processing of the images from physical sections was identical, except that the images were first aligned. The alignment was achieved with the freely downloadable software Reconstruct (Fiala 2005). The successive images were superimposed by aligning their common structures step by step on each image. The data stored in Reconstruct files were imported into Matlab for further analyses. In particular, the reconstructed brains were carefully checked to make sure that no distortion attributable to erroneous alignment was present. Indeed, the alignment procedure was precise from one image to the next but could lead to distortion at longer range. For this reason, several tests were performed by using different alignment procedures and by visualising each brain in planes different from the sectioning plane (i.e. parallel to the sagittal plane in one of the brains and perpendicular to it in the other brain). We checked that the sagittal plane was actually a plane and not a wavy surface. We found no evidence of distortion caused by incorrect alignments.

Standardisation of morphometrical data

In order to study quantitatively the invariant and variant features of the AL organisation, the original coordinates were standardised. The standardisation procedure involved data reduction, correction of differences in brain and AL orientations, correction of size differences and correction of overall differences in AL shapes.

Glomerular data reduction The coordinate system used for segmentation was defined by the orientation of the (optical or physical) sectioning plane. The x and z axes corresponded to the bottom and left edges of each image, respectively. The y axis corresponded to the succession of the intersections of x and z axes, at bottom-left, and defined the location of every section within the stack. In the reconstruction programs, biological structures are described as polyhedral surfaces. The coordinates of points on these surfaces give an accurate description of the shape and size of the structures but are relatively difficult to handle and not well adapted to the analyses presented here. As glomeruli are relatively regular subspherical structures, there are mostly advantages, from a computational point of view, to approximate them by spheres. The volume v and the coordinates x, y, and z of the centre of mass of each glomerulus were calculated from its outlines. The data relative to a glomerulus were then reduced to four values: the coordinates x, y, and z and the radius r of the sphere having the same volume, with $r = (3v/4\pi)^{1/3}$.

Up to this point, the use of available standard software, e.g. Amira or Reconstruct, is advantageous. However, all subsequent operations (standardisation and morphometrical analyses) apply to ensembles of spherical objects or points (centres of spheres) representing glomeruli whose handling requires specific algorithms. These algorithms are not available in standard packages. Although their integration in Amira and Reconstruct is possible and desirable, it proved faster to develop and test them as independent Matlab toolboxes (available on demand). For this reason, coordinate data from Reconstruct were exported to Matlab for the treatments described below.

Non-rigid transformation ALs may deviate from spheres and resemble ellipsoids. Therefore, ALs were "sphericised" by anisotropic scaling with different scaling factors along three orthogonal directions. Scaling factors were normalised in order to preserve volume. The scaling axes and factors were determined from the covariance matrix of the glomerular coordinates. This transformation corresponds to a "sphericisation" of the AL because the AL elongation is now the same in all directions.

Rigid transformations The coordinates of glomeruli were initially expressed in a system xyz of axes defined with respect to the sectioning plane (and image stack), not to the brain. In order to compare ALs, translations, reflections and rotations were performed. In intra-individual comparisons, rotations were used in order to compensate for lack of symmetry, whereas for inter-individual comparisons, rotations were required to correct the inter-individual variability of the sectioning plane and image stack orientations. After these transformations, the initial x, y and z coordinates were expressed in a system XYZ of conventional neuroanatomical axes (Strausfeld 1976), with X being latero-lateral, Y antero-posterior and Z ventro-dorsal (Fig. 1). Two types of registrations were used: the first for intra-individual comparisons, the second for inter-individual comparisons.

For intra-individual comparisons, a first translation made the middle point of the right and left AL centres the origin of the axes. By a reflection with respect to the sagittal plane, the reflected AL is expected to coincide with the other AL. Such a reflection is obtained by inverting the sign of a single coordinate provided the sagittal plane contains the two other coordinate axes. To meet this condition, the coordinate axes were rotated such that the x axis was parallel to the line joining the centres of the right and left ALs. After such a rotation, the x axis coincides with the medio-lateral X axis and the sagittal plane is approximately parallel to the plane containing the y and z axes. When this was insufficient to obtain a symmetrical representation of the right and left ALs, we searched a global rotation of one AL around an axis going through its centre, the other AL

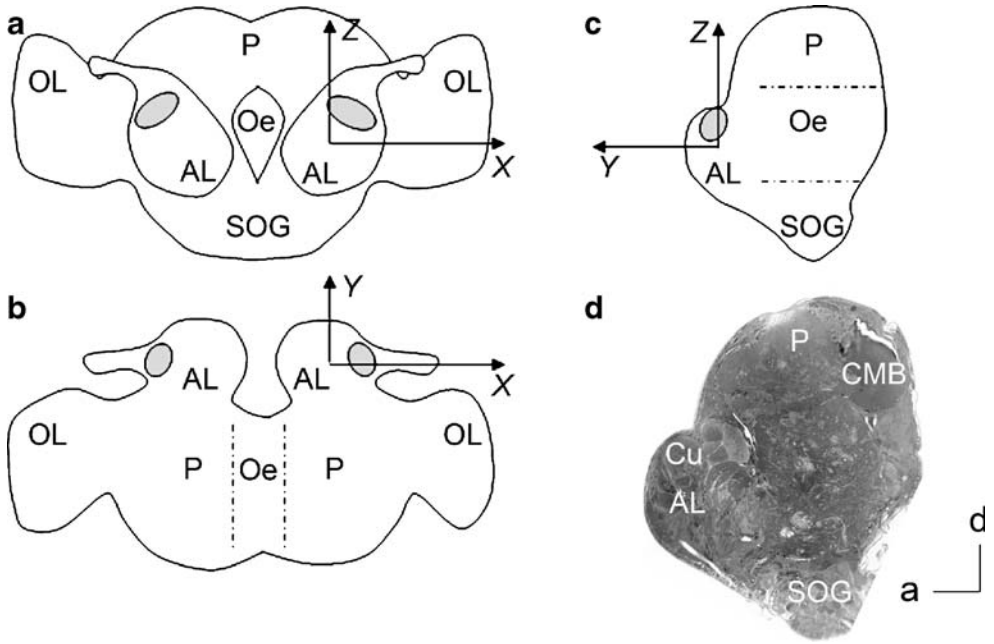

Fig. 1 Anatomical axes used to define the standard coordinates of glomeruli, shown on anterior (**a**), dorsal (**b**) and sagittal (**c**) views of the brain. The axes are such that, if the right and left antennal lobes (ALs) are perfectly symmetrical, homologous glomeruli will have identical coordinates. For each AL, the origin of coordinates is at the centre of gravity of its glomeruli. The three axes are orthogonal to one another, with *X* being medio-lateral along the line connecting the centres of both ALs, *Y* being antero-posterior and *Z* being ventro-dorsal (*AL* antennal lobe, *Oe* oesophagus, *OL* optical lobe, *P* protocerebrum, *SOG* sub-oesophageal ganglion). **d** Sagittal section of ethyl-gallate-stained brain slm1, equivalent to **c**, showing the orientation of *Y* and *Z* axes (*a* anterior, *Cu* cumulus, *d* dorsal, *CMB* calyx of the mushroom bodies). *Bars* 100 μm

remaining fixed, thereby enabling the recovery of the right-left symmetry (Fig. S1 in Electronic Supplementary Material). We determined both the axis and the angle of rotation by an optimisation method (Nelder-Mead simplex algorithm) minimising the sum of squared-distances between a set of homologous glomeruli identified in both ALs. Then, to simplify the comparisons, we adopted the convention of considering the mirror image of the left AL, so that corresponding (symmetrical) glomeruli in both ALs were now superimposed, and we took the right AL centre as the origin of the coordinate system. An average AL was computed by averaging the coordinates and the radii of the glomeruli from the right and the reflected left ALs.

Inter-individual comparisons were performed on average ALs from two different brains. The *X* axes of both brains being the same, ALs were registered by using essentially a rotation (angle γ) around *X* and smaller rotations around the other two axes, optimising the coincidence of landmarks in both brains (Fig. S2 in Electronic Supplementary Material). The final coordinates after rotation are denoted *X*, *Y* and *Z*.

Standardised representations A convenient representation of an AL is a two-dimensional graph showing the AL as seen by an observer located on the six standardised half-axes and, for this reason, being identical in all individuals. An observer located on the latero-lateral *X* axis, either on the lateral *X*+ or the medial *X*- half-axes, sees two sagittal views of the AL (sagittal plane *YZ*). An observer on the antero-posterior *Y* axis, looking at the AL from an anterior (on *Y*+) or posterior (on *Y*-) point, sees two frontal views (frontal plane *XZ*). Finally, two horizontal views picture the *XY* dimensions of the AL for an observer looking from either a dorsal (*Z*+) or a ventral (*Z*-) position. We term these series of six views drawn according to the fixed axes *X*, *Y* and *Z* as "standardised representations" of ALs.

Standardised representations captured glomeruli as spheres or with a realistic shape computed earlier by surface reconstruction. Standardised spherical representations had the advantage that "average ALs" could be computed easily. In order to assess inter-individual variability, pairwise comparisons of the five AL averages were performed.

Visual identification of glomeruli

As mentioned above, some glomeruli could be recognised as being homologous, in all 10 (six ethyl-gallate-stained and four synapsin-stained) ALs, directly on sections. These characteristic units were referred to as landmark glomeruli.

With these landmarks as a starting point, progressively more neighbouring glomeruli were identified by the characteristic patterns that they formed until most glomeruli had been visually attributed a contralateral homologue. This was performed on all available types of representations and the results were compared to ascertain that no mismatch appeared. The same process was applied inter-individually. When all homologies were found, the same number was attributed to the homologous glomeruli in the 10 ALs. The glomeruli were numbered along the *Y* axis, with G01 being the most anterior and G63 the most posterior.

Morphometric analyses

Comparison of size and location of visually homologous glomeruli The histograms of radii within each AL were compared with normal distributions by the Kolmogorov-Smirnov test. Pearson's coefficients of correlation r between the radii and between the locations of the visually homologous glomeruli were tested based on their standard normalised version $r((n-2)/(1-r^2))^{1/2}$, which follows Student's distribution (Snedecor and Cochran 1967) for any pair of non-correlated Gaussian variables. For location, the coordinates X, Y and Z and the distance D between each glomerulus and the centre of the AL, $D=(X^2+Y^2+Z^2)^{1/2}$, were used as measures of location and plotted against the same measure for the visual homologue. If visual homologues had exactly the same spatial position and size, the plotted points would be aligned and the coefficients of correlation would be 1.

Computational nearest-neighbour pairing of glomeruli based on their spatial location The precision of the spatial location of glomeruli across ALs was also assessed by using an algorithm for computational pairing as described earlier (Rospars and Chambille 1981). Briefly, this algorithm uses the standardised coordinates to compare the relative location of glomeruli belonging to different ALs, independently of the visual pairing. For each given glomerulus A in an AL "a", the glomeruli belonging to the compared AL "b" are sorted by distance to A. The closest glomerulus in AL "b" is called the first counter-neighbour. Two glomeruli A and B are considered as matched if they meet the following criteria of uniqueness and reciprocity (Rospars 1983): A should be the closest counter-neighbour of B and of no other glomerulus and, symmetrically, B should be the first counter-neighbour of A and of no other glomerulus. This analysis was made iteratively. At the initial iteration, a global superimposition was used putting into coincidence the centres of gravity of all glomeruli in both ALs. Then, at the next iterations, only pairs found at the previous iteration were used. For each glomerulus A, a specific local superimposition was performed based on the centres of gravity of the small sets of glomeruli located within a sphere of radius 54 μm (i.e. twice the average glomerular radius) centred on A, provided that these glomeruli were matched at the previous iteration. This procedure took into account local displacements of groups of glomeruli. The iterations were stopped when they brought no further increase in the number of matched glomeruli. The difference of the number of pairs between the first (global) and last iterations provided an estimate of the importance of the local displacements.

Results

Organisation of antennal lobes

The AL of *S. littoralis* occupies approximately 1.66×10^7 μm^3. A sphere of equivalent volume would have a radius of ca. 160 μm. Glomeruli are distributed in approximately one layer around a coarse fibrous core (Fig. 2a). The cell bodies form a bulky lateral cluster and a smaller medial one. The neural processes originating from the lateral cluster cross the peripheral layer of the glomeruli and join the central fibrous core; this results in a lateral gap in the glomerular layer (Fig. 2c). The tract from the medial cell cluster also interrupts the peripheral layer of the glomeruli medio-dorsally, although this tract is less visible as the number of cells in the cluster is much smaller (Fig. 2c). These gaps separate the main ventro-medial cluster (VMC) of glomeruli from a smaller dorso-lateral cluster (DLC), which includes the cumulus G18 and a dozen other glomeruli (Fig. 2c).

Visual identification of glomeruli

Segmentation A complete description of the AL glomerular architecture was performed, based on six ethyl-gallate-stained ALs from three animals and four synapsin-stained ALs from two animals (Fig. 3). We counted 60–63 glomeruli in the ethyl-gallate-stained ALs (Table 1). Smaller numbers were found in the two synapsin-stained brains (respectively, 57–57 and 57–55 glomeruli in the left and right ALs; Table 1) because the deepest optical sections proved difficult to segment reliably. For this reason, the ethyl gallate preparations were taken as a reference and the total number of glomeruli was estimated as close to 63. However, the significance of this number could be established only after individual identification of the glomeruli.

Description of glomerular patterns Twenty glomeruli, referred to as "landmark glomeruli", were identified directly from the serial sections, either from their closeness

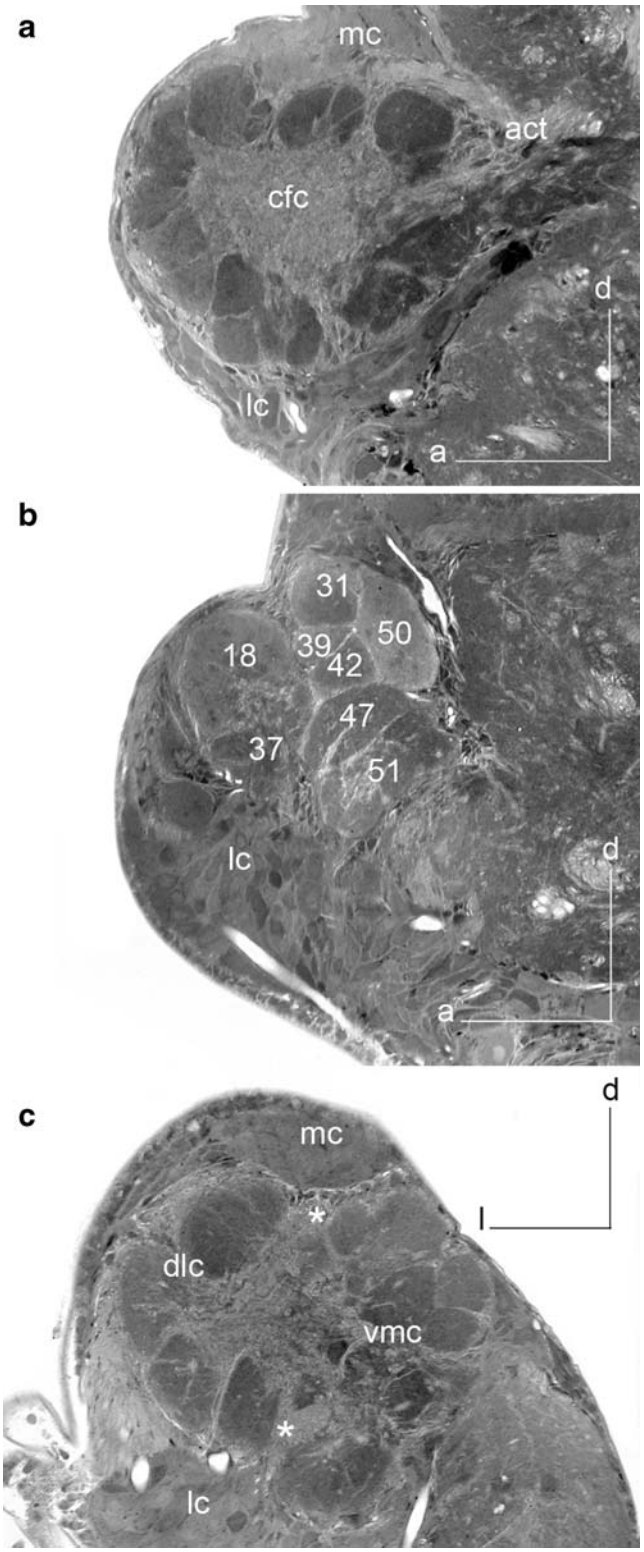

Fig. 2 Ethyl-gallate-stained 5-µm-thick sections of the brain in male *Spodoptera littoralis*. **a**, **b** Sagittal sections across the AL in preparation slm1. **a** The AL was cut at its maximum diameter and appears almost spherical (*a* anterior, *act* antenno-cerebral tract, *d* dorsal). Two main cell body clusters are visible laterally and medially (*lc* lateral cluster of cell bodies, *mc* medial cluster of cell bodies). The glomeruli are distributed in a single layer around a central fibrous core (*cfc*). **b** The AL has been cut close to the antennal nerve, revealing the typical pattern formed by the glomeruli of the dorso-lateral cluster. A row of medium and small glomeruli (*31*, *39*, *42*, *47*, *51*) is sandwiched between the two large antennal-nerve glomeruli (*18*, *37*) anteriorly and by G50 (*50*) posteriorly. **c** Frontal section across the AL of slm2 showing the two gaps that separate the dorso-lateral (*dlc*) from the ventro-medial cluster (*vmc*) of glomeruli (*stars* lateral and medial gaps neighbouring, respectively, the lateral and medial clusters of cell bodies, *l* lateral). *Bars* 100 µm

to easily recognisable non-glomerular landmarks or on the basis of the characteristic patterns that they formed with one another. The non-glomerular landmarks that we used were the antennal nerve (AN), the medial and lateral clusters of cell bodies (MC and LC) and the tracts connecting the AL to the protocerebrum (Figs. 2, 3). Most landmark glomeruli belonged to the posterior AL and, more specifically, to the DLC.

The first ten landmark glomeruli belong to the DLC and are easily recognised based on their location and the pattern that they form. The cumulus of the MGC (macroglomerular complex; G18) is located at the AN entrance. It has a bean-shaped frontal section and is the largest glomerulus with an average radius of 42 µm, which reflects dimensions of 54×73×96 µm (dorso-lateral to ventro-medial, antero-posterior and ventrolateral to dorsomedial dimensions, respectively). It is flanked medio-ventrally by G37 and medio-dorsally by G17 (Figs. 3d, j, 4b, h). G37 is in the same size range, with an average radius of 32 µm. G17 is smaller with an average of 28 µm in radius. Immediately posterior to these first three is a row of six glomeruli, namely G51, G47, G42, G39, G31 and G40, following a ventro-dorsal progression (Figs. 3f, l, 4a, g). G51 and G47 mark the ventral limits of the DLC (Fig. 4e, k). The row of glomeruli is sandwiched between G18 and G37 anteriorly and G50 posteriorly (e.g. Figs. 2b, 4a, g). G40 and G50 form the dorsal border of the DLC (Figs. 2b, 4e).

Other landmark glomeruli have been identified based on their location relative to the tracts. G59 is one of the posterior-most glomeruli of the AL (Figs. 3f, 4c, i, f, l) and surrounds tracts exiting the AL (Fig. 4e). G57 and G63 lie ventral to the lateral gap; thus, they constitute the dorso-lateral limit of the VMC (Figs. 3e, f, 4b, e, k). In addition, they are separated from G59 by a tract. G54, G52 and G56 constitute the dorso-medial border of the VMC (Fig. 4e, k); they also have a typical location in between two tracts (Fig. 3f). At more anterior levels compared with this group of three, the dorsal border of the VMC is lined with glomeruli G30 and G45 (Figs. 3e, 4c, i); both have a stable location with respect to the median gap. Finally, two more glomeruli have characteristic locations with respect to the lateral gap: G55 and G46 are found anterior to G57

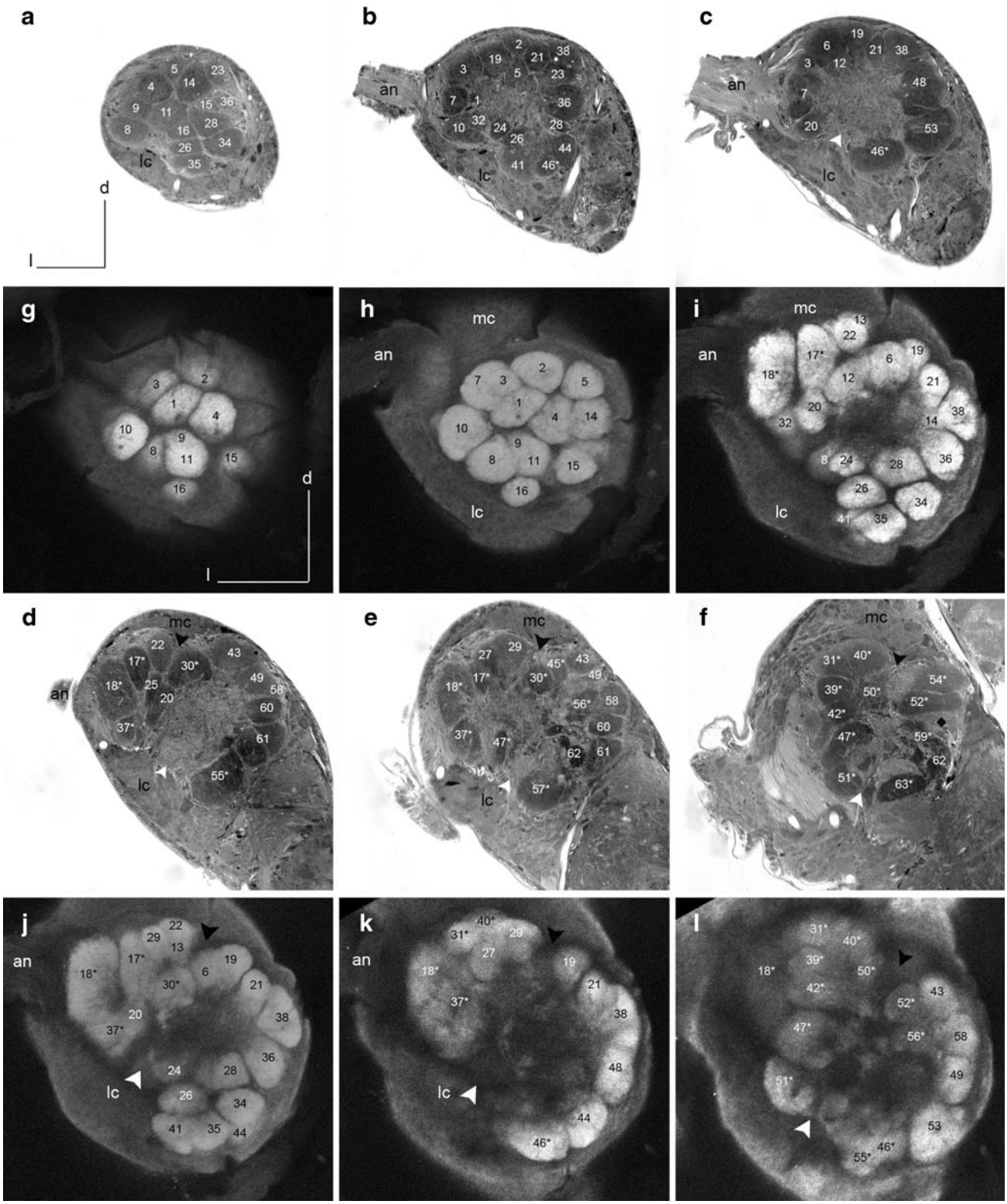

and G63 (Fig. 4f, l) and mark the postero-lateral limit of the VMC. G55 and G46 are also noticeable by their relatively large size of, respectively, 31 and 26 μm in radius.

Visual pairs With these landmark glomeruli as a starting point, progressively more and more neighbouring glomeruli were identified by the patterns that they formed with the former. These patterns were systematically sought in three-

◀ **Fig. 3** Parafrontal sections through ALs of *S. littoralis* at various depths along the antero-posterior *Y* axis. **a-f** Ethyl gallate staining of serial sections (respectively, sections 11, 19, 24, 32, 38 and 46) observed by standard light microscopy; animal slm2. Sections (5 μm thick) were chosen to show the complete set of glomeruli in this AL. Apart from glomeruli G13 and G33, which were not present in the imaged AL, all glomeruli appear at least on one section (*an* antennal nerve, *lc* lateral cluster of cell bodies, *mc* medial cluster of cell bodies, *stars* landmark glomeruli, *white arrowheads* lateral gaps, *black arrowheads* medial gaps, *black lozenge* secondary tract delimiting the group G54, G52, G56, *d* dorsal, *l* lateral). **g-l** Synapsin-stained whole-mount optically sectioned (at 3.2 μm; respectively, optical sections 7, 15, 26, 30, 38 and 46) by confocal microscopy; right AL of animal slm5. The sections were chosen to match the physical sections in **a–f** as closely as possible, in spite of the differences in sectioning plane. These sections illustrate the difficulty of identifying homologous glomeruli in different brains, even when sectioning planes are not very different. Some glomeruli (G25, G33, G45, G59, G62, G63) could not be delineated on this preparation. Other glomeruli (G23, G54, G57, G60 and G61) are present but are not shown on the selected sections. However, most are shown on the AL reconstruction (see Fig. 4). *Bars* 100 μm

dimensional reconstructions by comparing first the right and left ALs of each brain and then the ALs of different brains until most glomeruli were visually identified. In intra-individual comparisons, we found 56 and 54 pairs for the two optically sectioned brains (slm4 and slm5, respectively) and 62, 58, 59 pairs in the physically sectioned brains (slm1–3; Table 2). Thus, this step yielded an average rate of pairing of 85%–89% in the former and 94%–98% in the latter, taking 63 as the total number of glomeruli. The visual inter-individual pairing produced 45 (71%) pairs common to all five brains, whereas 12 were common to four brains and five to three brains or less (see Table 1).

Anomalous glomeruli Some glomeruli could not be found in both ALs of the same brain, even in the best resolved preparations (ethyl gallate). A single asymmetric glomerulus was found in slm1 (G32), three in slm3 (G25, G09, G32) and four in slm2 (G27, G35, G26, G33). The glomeruli absent in both ALs of a brain were rarer: none was found in slm1 and only one in slm2 (G13). G33 was found in three ALs only, bilaterally in slm1 and in the left AL of slm2 (Fig. 4h). No supernumerary glomerulus, i.e. present bilaterally in a single brain, was found.

Spatial location of identified glomeruli

The respective contribution of constancy and variability in the spatial organisation of the glomerular array can be assessed only through quantitative analyses. These analyses demand that glomerular coordinates be expressed in a standard coordinate system, identical for all ALs. Inter-individual comparisons were performed by using one average AL per individual (see Materials and methods). Whenever a glomerulus remained unpaired through the intra-individual comparison step, it was left out of the average AL.

The deviations from identical positions of visually paired glomeruli were displayed by using regression plots of their standard coordinates and their distances to the AL centre (Fig. 5) and plots of the distances between visually paired glomeruli (Fig. 6). Quantitative criteria were used to complement these plots, namely the coefficients of correlation of the coordinates and distances for visual pairs, the mean distances between glomeruli of the same visual pair and the search of ambiguous and unambiguous visual pairs based on the nearest-neighbour computer algorithm, which used only spatial coordinates. All these criteria were found to depend on the nature of the comparison (intra- or inter-individual) and on global corrections of the orientation and shape of the ALs.

For visually paired glomeruli, the coefficients of correlation of the coordinates and distances to the AL centre were found to be similar for intra-individual (between 0.70 and 0.87, Table 3, Fig. 5a) and inter-individual comparisons (0.70 and 0.89, Table 3, Fig. 5b). The distances between homologues were in the range of 16 to 29 μm in the same brain (Table 2) and 17 to 25 μm across brains (Table 3).

Regarding the nearest-neighbour pairing scores, 36–45 pairs were obtained in intra-individual comparisons; this represented an average of 69% of the glomeruli matched by computation only. Between two and six pairs were matched in a different way by visual and computational pairing, with 12–25 glomeruli remaining unmatched (Table 4). The nearest-neighbour inter-individual pairing scores yielded 26–50 pairs, involving 57% of the glomeruli on average (Table 5). Among these pairs, one to six differed from those proposed visually, which left an average of 51% of the glomeruli unambiguously identified. Twenty-four glomeruli were consistently identified as homologues by the algorithm, throughout seven or more of the ten inter-individual comparisons (Fig. 7).

The comparisons summarised above (Tables 2, 3, 4, 5) were obtained on normalised coordinates, i.e. after correction of the differences in orientation and shape of the ALs. The same approach was utilised to assess the importance of this normalisation by comparing the values of the mean characteristics for visual and computational pairs before and after normalisation (Table 6). This showed that the effect of normalisation was always positive and improved glomerular pairing.

Two kinds of variations could be distinguished: those that affect glomeruli without hiding their correspondence in different ALs and those that introduce ambiguity in their identification. We document here four types of displace-

Table 1 List of glomeruli missing in at least one AL

Missing glomeruli[a]		Ethylgallate-stained ALs						Synapsin-stained ALs				n_1[b]	n_2[c]
		slm1		slm2		slm3		slm4		slm5			
		Right	Left	Right	Left	Right	Left	Right	Left	Right	Left		
Unilaterally (always)	9	x	x	x	x	x	-	x	x	x	x	1	0
	26	x	x	x	-	x	x	x	x	x	x	1	0
	27	x	x	x	-	x	x	x	x	x	x	1	0
	35	x	x	x	-	x	x	x	x	x	x	1	0
	42*	x	x	x	x	x	x	x	x	-	x	1	0
	43	x	x	x	x	x	x	x	-	x	x	1	0
	45*	x	x	x	x	x	x	x	x	-	x	1	0
	55*	x	x	x	x	x	x	x	x	x	-	1	0
	57*	x	x	x	x	x	x	-	x	x	x	1	0
	63*	x	x	x	x	x	x	x	x	-	x	1	0
	32	-	x	x	x	-	x	x	x	x	x	2	0
Bilaterally (sometimes)	13	x	x	- B -		x	x	x	x	x	x	2	1
	30*	x	x	x	x	x	x	- B -		x	x	2	1
	39*	x	x	x	x	x	x	x	x	- B -		2	1
	59*	x	x	x	x	x	x	- B -		- B -		4	2
	62	x	x	x	x	x	x	- B -		- B -		4	2
	25	x	x	x	x	-	x	- B -		- B -		5	2
	33	x	x	-	x	- B -		- B -		- B -		7	3
Number of missing		1	0	2	4	3	2	6	6	8	6		
Total number[d]		62	63	61	59	60	61	57	57	55	57		
Bilaterally missing		0		1		1		5		5			
Total per animal[e]		63		62		62		58		58			

*Landmark glomeruli are present in the six ethylgallate-stained ALs

[a] Glomeruli (18) either present (*x*) or absent (-); all others (45) present in all 10 ALs studied.

[b] n_1 Number of ALs in which the listed glomerulus is missing

[c] n_2 Number of animals in which the listed glomerulus is missing bilaterally (- B -)

[d] Total number of delineated glomeruli per AL=63−number of missing

[e] Total number of glomeruli per animal (bilaterally missing not counted)

ments of the first category, namely the differential expansions of ALs in three orthogonal directions, the differential rotations of ALs around their centres, the small local displacements of groups of neighbouring glomeruli and the random fluctuations decreasing the bilateral symmetry. The four types of displacements share the common property that they can be corrected: the first type without any identification of glomeruli, the second type on the basis of only a few identified glomeruli used as landmarks, the third type by the local mode of the nearest-neighbour algorithm and the last type by averaging the coordinates of visually homologous glomeruli in the right and left ALs of the same brain. The first two types are clearly apparent in the significant improvement of the quantitative characteristics describing the overall similarity of the compared ALs (e.g. distances between visual pairs, correlations of coordinates, number of nearest-neighbour pairs) after the corrections are performed. Their influence is most remarkable in the case of slm3 (Fig. S1 in Electronic Supplementary Material). The remaining displaced glomeruli after the mentioned corrections result in 31%–32% ambiguous pairs for intra-individual (Table 4) and 41%–46% for inter-individual (Table 5) comparisons.

Size of identified glomeruli

The size of glomeruli was calculated as the radius of the sphere with the same volume. No normalisation was

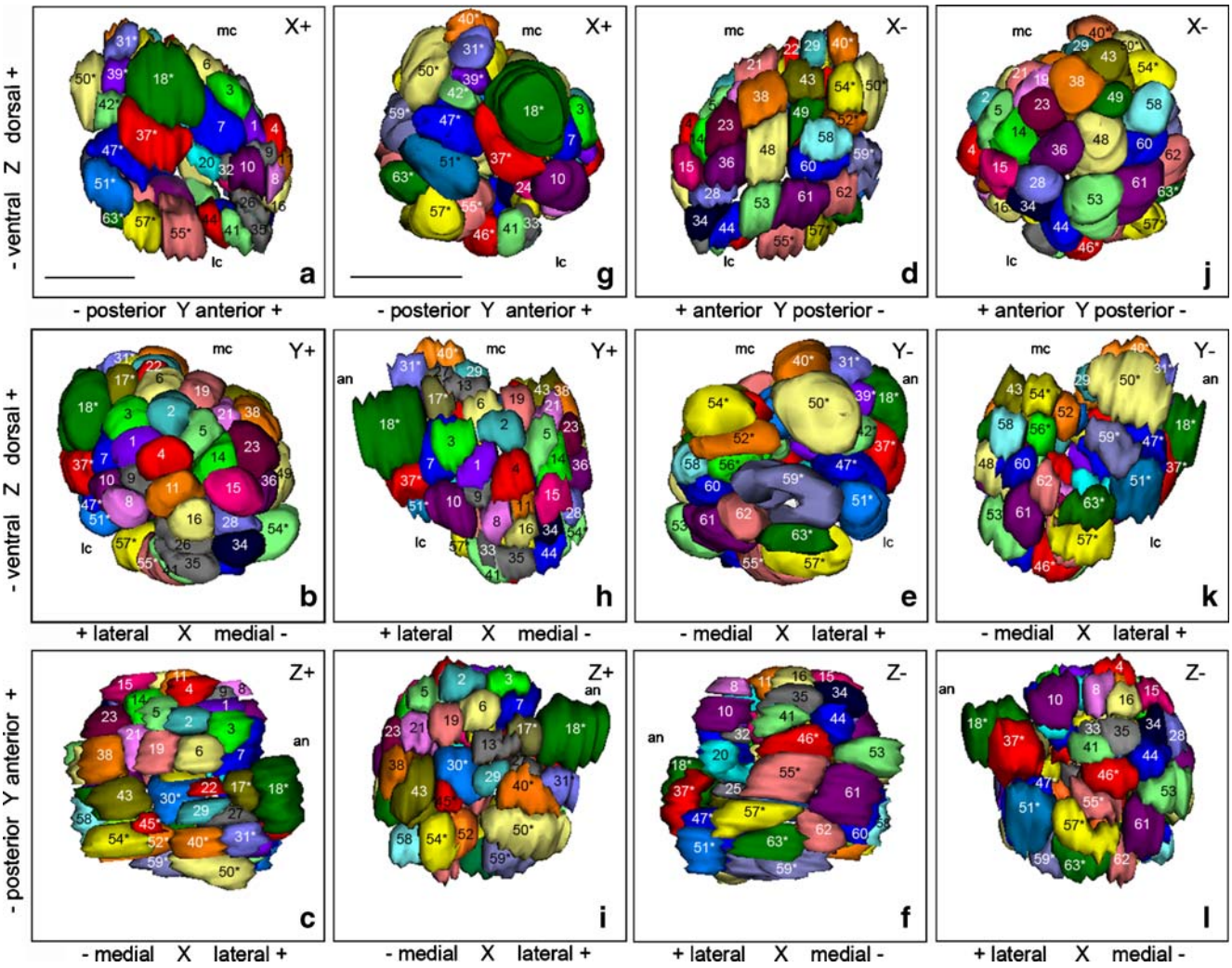

Fig. 4 Reconstructions of non-normalised ALs in male *S. littoralis* shown from six standard viewpoints. The reconstructions are based on ethyl-gallate-stained ALs, from slm2 (**a-f**) and slm1 (**g-l**), respectively sectioned parafrontally and parasagitally. G13 and G33 are not present in this AL of slm2, whereas other glomeruli (G12, G24) are present but are not tagged because of their hidden position in the glomerular layer. In slm1, G32 and G25 are not present and G26, G22, G20 and G12 are hidden by other glomeruli (*stars* landmark glomeruli, *grey* anomalous glomeruli, *an* antennal nerve, *lc* lateral cluster of cell bodies, *mc* medial cluster of cell bodies). *Bars* 100 μm

applied. The correlation between radii of visually homologous glomeruli was between 0.76 and 0.94 within each brain (Table 2, Fig. 8a, b) and between 0.65 and 0.90 across brains (all tests highly significant, Table 3, Fig. 8c, d).

The radii ranged from 14 to 47 μm, with a mean value of 27 μm. Their distribution was approximately Gaussian (Fig. 9). The largest glomerulus, G18, was at three standard deviations from the mean and was about five times as voluminous (380,000 μm^3) as the average glomerulus (82,500 μm^3). No regular size gradient could be observed in the AL but the largest glomeruli always showed similar locations: close to the AN (G17, G18), posterior (G47, G50, G51, G59) and medio-ventral (G38, G48, G53, G55, G57, G61).

Discussion

Constancy and variability in AL of *S. littoralis*

Previous studies in many insect orders based on neuroanatomical, functional and molecular techniques have provided evidence of the stable identity of glomeruli in a given species, sex and developmental stage (see Rospars 1988; Huetteroth and Schachtner 2005; also other references given in the Introduction). The standard interpretation at present is that glomerular identity results ultimately from the termination of ORNs expressing the same OR in each glomerulus and only a few exceptions have been documented (Hallem et al. 2006). Although qualitative and quantitative arguments point

Table 2 Intra-individual comparisons of the position and dimension of visual pairs of glomeruli

Comparison[a]	St[b]	To_R[c]	To_L[c]	N_v[d]		d_v[e]	Cor_D[f]	Cor_R[g]
1R-1L	E	62	63	62	99%	21.85±8.31	0.79	0.90
2R-2L	E	61	59	58	97%	28.42±12.17	0.73	0.80
3R-3L	E	60	61	59	98%	29.29±14.61	0.70	0.94
4R-4L	S	57	57	56	98%	16.98±9.25	0.85	0.83
5R-5L	S	55	57	54	96%	16.02±8.28	0.87	0.76
Mean		59	59.4	57.8	97.6%	22.49±10.50	0.79	0.84

[a] Comparison of right AL (*R*) with left AL (*L*) in indicated brains (slm1to slm5)

[b] Staining and sections (*St*): ethyl gallate and physical (*E*) or synapsin and optical (*S*)

[c] Total number of glomeruli delineated in right (To_R) and left (To_L) ALs

[d] Number of visual pairs (N_v) between ALs and percentage with respect to mean of To_R and To_L

[e] Mean±SD of distances (d_v, in μm) between glomeruli of the same visual pair

[f] Coefficient of correlation between the distances of glomeruli to the AL centre of the same visual pair (Cor_D). All *P*-values<10^{-9} for the tests of the coefficients of correlation against null hypothesis, $r=0$

[g] Coefficient of correlation between the radii of glomeruli belonging to the same visual pair (Cor_R). All *P*-values<10^{-10} for the tests of the coefficient of correlation against null hypothesis, $r=0$

clearly to an underlying constancy of the glomerular array in insects, we have found that clear quantitative deviations from perfect invariance occur in the AL of *S. littoralis*. An initial discussion of the nature, extent and significance of these deviations is provided below and calls for further investigations in the future.

These two related questions of the constancy and variability of the ALs are important for neurophysiological investigations because many problems in olfactory coding rely on the proper identification of the glomeruli involved in a given function. From this point of view, the glomerulus occupies a favourable position in the hierarchical brain organisation because it lies at an intermediate level between the cellular level and the global network level. Therefore, the glomerular features may reveal characteristics of their underlying neural network. These features are discussed below with regard to number, size and position of glomeruli.

Number and identifiability of glomeruli

Constancy Although the exact number of glomeruli is probably the most difficult characteristic to establish reliably, we conclude, from our results, that the AL in *S. littoralis* is constituted of 63 glomeruli. Indeed, we have found this complement in only one ethyl-gallate-stained AL, the others being in the of range 60 to 62, with the synapsin-stained AL in the range of 55 to 57 (Table 1). The difference between counts from the different techniques comes from a loss of fluorescence in the deepest optical sections, as has also been mentioned in earlier studies (Masante-Roca et al. 2005; Sadek et al. 2002), and not from a true variation or from a diffuseness of the glomerular organisation in this area, as confirmed by physical sections and dorso-ventral scans of synapsin stained brains.

Variability We have tried to minimise the sources of experimental errors, such as the imperfect delineation of some glomeruli and the mismatching of glomeruli in three-dimensional reconstructions, by selecting the best available preparations and, in the case of preparations observed in confocal microscopy, by not including the unclearly resolved posterior glomeruli. Nevertheless, a few glomeruli might have been incorrectly delineated, which in turn might lead to difficulties in visual matching. However, we believe that, in the ethyl gallate preparations slm1 and slm3, these two kinds of errors can be considered as negligible. We base this conclusion on the consistent intra- and inter-individual visual matching. For these reasons, we believe that, in the later preparations, the variations observed are essentially of biological, not methodological, origin.

The variations of biological origin can take several different forms. In this subsection, we only consider those that affect the number of glomeruli and manifest themselves as anomalous glomeruli, either absent or supernumerary. We have found no example of a supernumerary glomerulus, i.e. present in only one animal. All anomalous glomeruli are absent, either on one side or on both sides of a brain. Both the presence of additional glomeruli and missing glomeruli in certain individuals have been found in the AL of other species (*M. brassicae*, Rospars 1983; *M. sexta*, Rospars and Hildebrand 1992, 2000; *Bombyx mori*, Kazawa et al. 2009). These anomalies can be tentatively interpreted as the lack

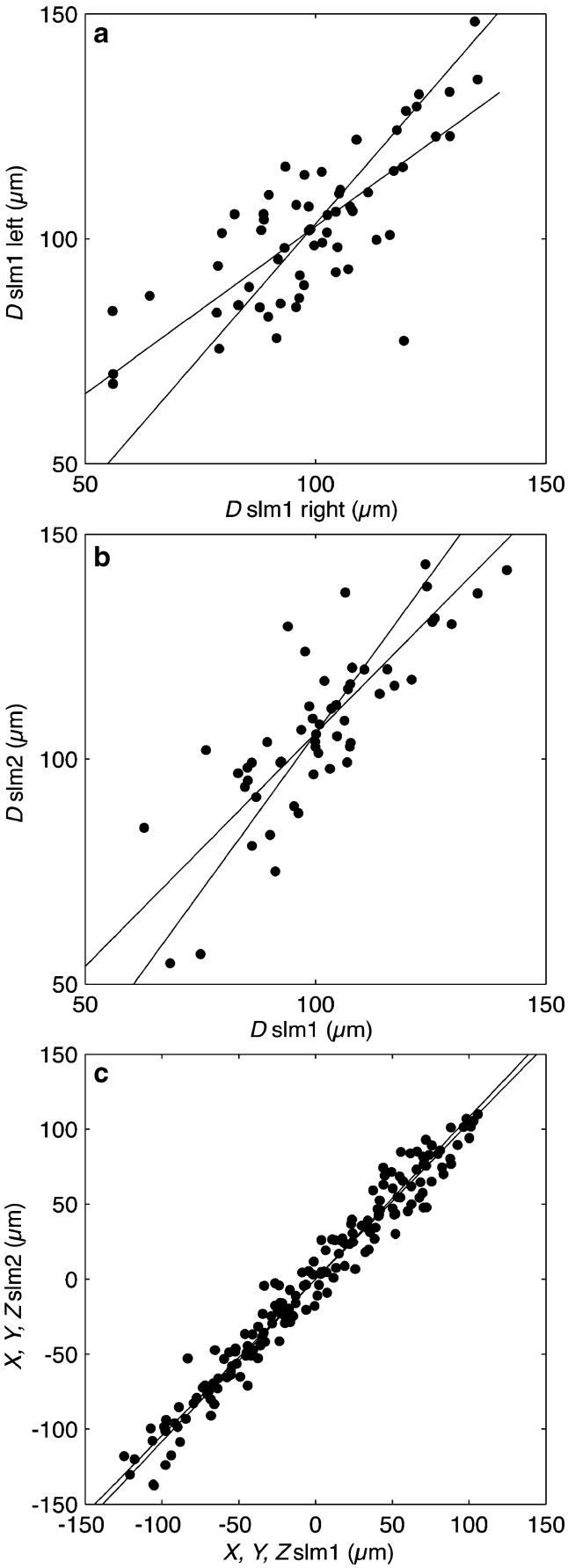

Fig. 5 Examples of scatter plots of normalised glomerular positions (distance *D* to AL centre). Intra- (**a**) and inter-individual (**b**, **c**) comparisons of visually paired glomeruli. **a** Distance *D* to AL centre of each right glomerulus of brain slm1 plotted against the distance to the AL centre of its visual homologue in the left AL. **b** Mean distance *D* of each right-left pair of brain slm1 plotted against the mean distance of the visually corresponding pair of glomeruli in slm2. **c** Same representation for all normalised coordinates (*X*, *Y*, *Z*) of each glomerulus. Regression lines *x/y* and *y/x* are shown. All coefficients of correlation are highly significantly different from zero (see also Tables 2, 3)

of expression of an OR gene or as an anomaly during development. We can speculate that the effect of these missing glomeruli on olfactory coding depends on the relative importance of the information normally coded by the missing OR(s) for the animal; this in turn depends upon the biological importance of the odorants interacting with these ORs and whether other ORs can detect these odorants.

Comparison between species and significance of number of glomeruli The AL in male *S. littoralis* has an organisation similar to that described in other moth species: a monolayer of glomeruli distributed around a central fibrous core. The number of 63 glomeruli found in *S. littoralis* is close to the counts reported in other male Noctuidae, i.e. 67 in *Mamestra brassicae* (Rospars 1983), 62–66 in *Heliothis virescens*, *Helicoverpa armigera* and *H. assulta* (Berg et al. 2002; Skiri et al. 2005) and 66 in *Agrotis ipsilon* (Greiner et al. 2004), in Bombycidae, i.e. approximately 60 in *B. mori* (Kanzaki et al. 2003; Kazawa et al. 2009), in Sphingidae, i.e. 63 in *Manduca sexta* (Rospars and Hildebrand 2000) and in Tortricidae, i.e. 71 in *Lobesia botrana* (Masante-Roca et al. 2005) and 50 in *Cydia molesta* (Varela et al. 2009). With the possible exception of the Tortricidae, these numbers suggest that moths, despite their wide diversification, have a conserved number of olfactory receptors and physiological types of ORNs. Unfortunately, no information is available on the functional homology between glomeruli in the different moth species, except for a few glomeruli, most notably the cumulus of the MGC and the labial pit organ (LPO) glomerulus.

Some functionally identified glomeruli In *S. littoralis*, three glomeruli (denoted "a", "b" and "c") have been recognised as part of the MGC by means of cobalt backfills from antennal sensilla (Ochieng et al. 1995) and by calcium imaging (Carlsson et al. 2002). The large glomerulus "a" (the cumulus) is located at the entrance of the AN in the AL and receives projections from ORNs responding to the major component of the sex pheromone. The two other glomeruli receive projections from ORNs tuned to a behavioural antagonist ("b") and to the minor component

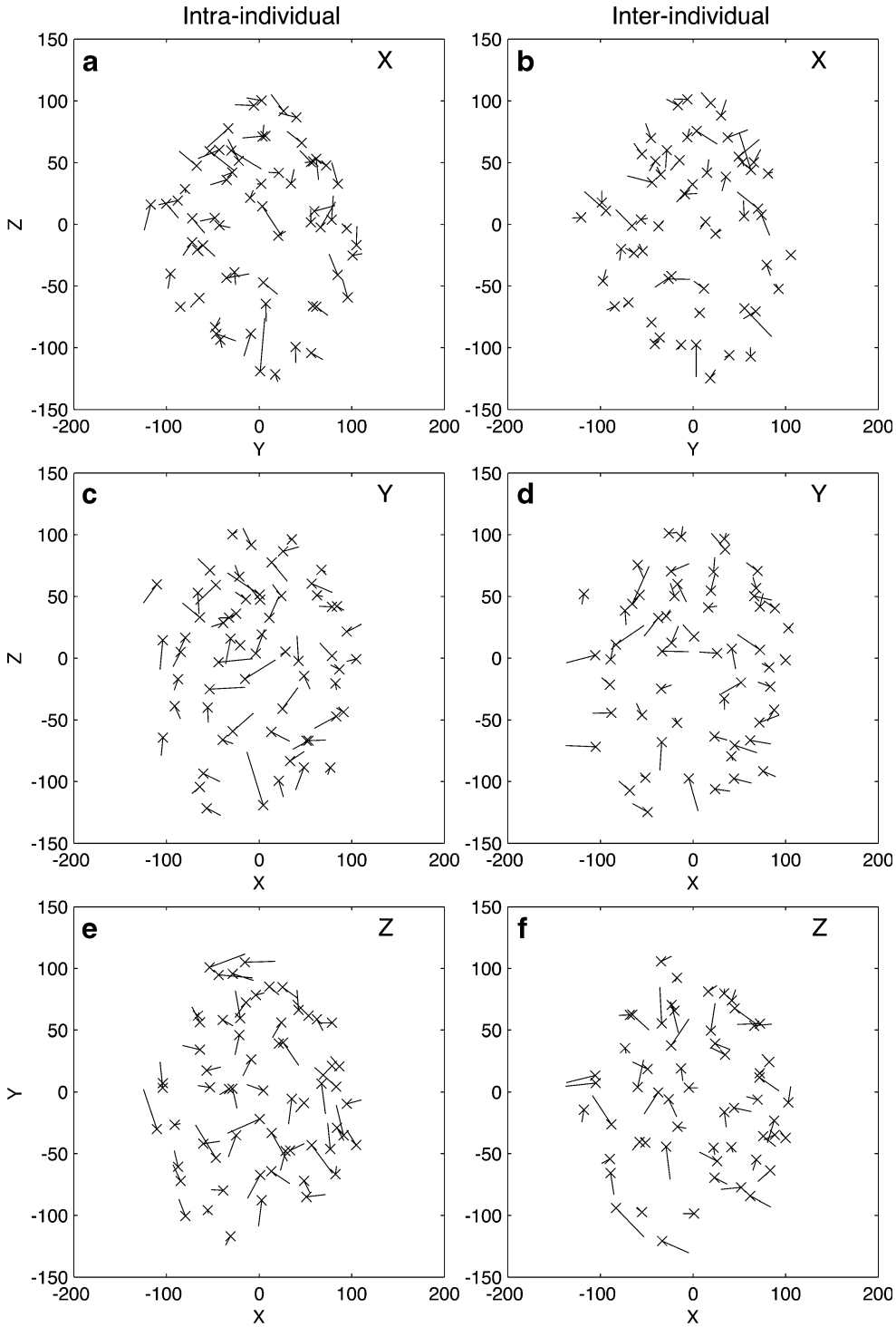

Fig. 6 Direct comparison of normalised glomerular coordinates. Intra-individual comparisons of slm1 right-left ALs (**a**, **c**, **e**) and inter-individual comparison of average ALs slm1-slm2 (**b**, **d**, **f**). Each segment joins the centres of two visually paired glomeruli with the *cross* on the right glomerulus (*left*) and slm1 glomerulus (*right*). From *top to bottom*, sagittal *YZ* (**a**, **b**), frontal *ZX* (**c**, **d**) and horizontal *XY* (**e, f**) planes

("c"). A fourth glomerulus, "d", is activated by another putative pheromone component and by other odorants (Carlsson et al. 2002) and the PNs arborising in it have been found to respond to pheromone components (Anton and Hansson 1995). From comparisons with the data published in these studies, G18 corresponds to "a", whereas G37 and G17 correspond to "c" and "b" respectively. We have not been able to identify the glomerulus corresponding to "d" unambiguously.

The shape, size and relative position of G53 (denoted as "F" in female *S. littoralis*; Sadek et al. 2002) suggest that it could be innervated by neurons from the LPO, as described in other species: receptor neuron projections from the LPO in moths and from maxillary sensilla in flies arborise uni- or

Table 3 Inter-individual comparisons of the position and dimension of visual pairs of glomeruli

Comparison[a]	St[b]	To_1[c]	To_2[c]	N_v[d]		d_v[e]	Cor_D[f]	Cor_R[g]
1M–2M	EE	63	62	57	91%	19.35±8.49	0.86	0.90
1M–3M	EE	63	62	59	94%	19.07±10.51	0.81	0.89
1M–4M	ES	63	58	55	91%	23.11±12.80	0.70	0.68
1M–5M	ES	63	58	53	88%	18.89±10.17	0.81	0.71
2M–3M	EE	62	62	55	89%	22.34±10.53	0.82	0.86
2M–4M	ES	62	58	52	87%	24.72±10.69	0.77	0.65
2M–5M	ES	62	58	50	83%	21.49±10.88	0.85	0.79
3M–4M	ES	62	58	54	90%	22.05±10.65	0.82	0.74
3M–5M	ES	62	58	52	87%	20.20±11.97	0.83	0.75
4M–5M	SS	58	58	51	88%	16.53±8.57	0.89	0.75
Mean		62.3	59.3	53.8	86.8%	20.78±10.53	0.82	0.77

[a] Comparison of average ALs of indicated brains (slm1 to slm5); *M* mean of right and left ALs

[b] Staining and sections (*St*): ethyl gallate and physical (*E*) or synapsin and optical (*S*)

[c] Total number of glomeruli delineated in first (To_1) and second (To_2) ALs in each comparison

[d] Number of visual pairs (N_v) between ALs and percentage with respect to mean of To_1 and To_2

[e] Mean±SD of distances (d_v, in μm) between glomeruli of the same visual pair

[f] All coefficients of correlation of distances to centre (Cor_D) highly significant with *P*-values<10^{-9}

[g] All coefficients of correlation of glomerular radii (Cor_R) with *P*-values<10^{-6}

bilaterally within one to three specific glomeruli in each AL (Kent et al. 1986; Guerenstein et al. 2004; Ignell et al. 2005; Ghaninia et al. 2007; Guerenstein and Hildebrand 2007). The large LPO glomerulus of *M. sexta* (Rospars and Hildebrand 1992, 2000) has also been identified because of its large size and ventral position in *H. assulta* and *H. virescens* (Berg et al. 2002).

Size of glomeruli

Constancy of glomerular size and its significance The objectivity of the identifications described above has been verified by their internal consistency and also by carefully checking the stability of the volume of the same glomerulus identified in different ALs. The high intra- and inter-

Table 4 Intra-individual comparison of the position of glomeruli by the nearest-neighbour algorithm in ALs of five male *Spodoptera littoralis*

Comparison[a]	To_R[b]	To_L[c]	App[d]		Id[e]		Dif[f]		Na_R[g]		Na_L[h]	
1R-1L	62	63	43	69%	41	66%	2	3%	19	30%	20	32%
2R-2L	61	59	39	65%	34	57%	5	8%	22	37%	20	33%
3R-3L	60	61	36	60%	30	50%	6	10%	24	40%	25	41%
4R-4L	57	57	45	79%	43	75%	2	4%	12	21%	12	21%
5R-5L	55	57	39	70%	37	66%	2	4%	16	29%	18	32%
Mean	59	59.4	40.4	69%	37	63%	3.4	5.8%	18.6	31%	19	32%

[a] Comparison of right AL (*R*) with left AL (*L*) in indicated brains (slm1 to slm5)

[b] Total number of glomeruli delineated in right AL ($To_R=App+Na_R$)

[c] Total number of glomeruli delineated in left AL ($To_L=App+Na_L$). All percentages in a row given with respect to mean of To_R and To_L

[d] Number of nearest-neighbour pairs found at the last iteration (*App*, see Materials and methods)

[e] Number of nearest-neighbour pairs identical to the visual pairs (*Id*)

[f] Number of nearest-neighbour pairs different from the visual pairs (*Dif*, *App=Id+Dif*)

[g] Number of glomeruli in right AL left unmatched by the nearest-neighbour algorithm (Na_R)

[h] Number of glomeruli in left AL left unmatched by the nearest-neighbour algorithm (Na_L)

Table 5 Inter-individual comparisons of the position of glomeruli by the nearest-neighbour algorithm in ALs of five male *S. littoralis*

Comparison[a]	To_1[b]	To_2[c]	App[d]		Id[e]		Dif[f]		Na_1[g]		Na_2[h]	
1M–2M	63	62	50	80%	47	75%	3	5%	13	21%	12	19%
1M–3M	63	62	37	59%	33	53%	4	6%	26	42%	25	40%
1M–4M	63	58	26	43%	22	36%	4	7%	37	61%	32	53%
1M–5M	63	58	30	50%	27	45%	3	5%	33	55%	28	46%
2M–3M	62	62	35	56%	33	53%	2	3%	27	44%	27	44%
2M–4M	62	58	34	57%	28	47%	6	10%	28	47%	24	40%
2M–5M	62	58	34	57%	29	48%	5	8%	28	47%	24	40%
3M–4M	62	58	27	45%	23	38%	4	7%	35	58%	31	52%
3M–5M	62	58	31	52%	28	47%	3	5%	31	52%	27	45%
4M–5M	58	58	41	71%	40	69%	1	2%	17	29%	17	29%
Mean	62	59.2	34.5	57%	31	51%	3.5	5.8%	27.5	46%	24.7	41%

[a] Comparison of average ALs of indicated brains (slm1 to slm5; *M* mean of right and left ALs)

[b–f] As in Table 4 (with *App=Id+Dif*). All percentages in a row given with respect to mean of To_1 and To_2

[g] Number of glomeruli in first AL left unmatched by the nearest neighbour algorithm (Na_1) with $App+Na_1=To_1$

[h] Number of glomeruli in second AL left unmatched by the nearest neighbour algorithm (Na_2) with $App+Na_2=To_2$

individual correlation coefficients (0.84, Table 2; 0.77, Table 3, respectively) for the sizes of glomeruli in the same visual pairs (Fig. 8) underline their constancy. The volume of glomeruli probably reflects the number of neurons and the density of arborisations within them. Hence, beyond confirming the correctness of visual identifications, the high coefficients of correlation obtained between individuals give additional evidence of the stability of their underlying neuronal organisation. In other insects, experience-dependent variability of glomerular size has been found (Devaud et al. 2003; Huetteroth and Schachtner 2005). In our study, however, the influence of experience can be excluded, because only freshly emerged males were used.

Variability and its interspecific variations The variability in size has been examined globally and on a per glomerulus basis. Only small differences in global AL size have been found between different individuals. The correlations in size of homologous glomeruli in intra- ($r\approx0.84$, Table 2) and inter-individual comparisons ($r\approx0.88$, ethyl gallate only, Table 4) are similar. This contrasts with previous observations showing that size is more variable between individuals than within an individual, as reported in *B. craniifer* ($r\approx0.85$ intra-individual, 0.5 inter-individual; Rospars and Chambille 1981) and *M. brassicae* ($r\approx0.90$ intra-individual, 0.82 inter-individual; Rospars 1983). If only experience-dependent effects were playing a role, we would expect that inter-individual variability is always higher than intra-individual variability, both ALs in a given individual being a priori exposed to the same odours.

Position of glomeruli

Constancy The analyses of glomerular position are based on statistical tests of the near equality of the normalised coordinates of glomeruli in the same visual pair (Tables 2, 3) and on an independent identification by using the nearest-neighbour algorithm (Tables 4, 5). These various tests give strong evidence for the identifiability of glomeruli. However, it is important that spatial invariance is made quantitatively clear only after normalisation of the coordinates.

Variability and its interspecific variations The comparison of raw and normalised data has revealed the presence of two main kinds of positional variability: those that can be corrected by sphericisation, rotations and local displacements and those that cannot be corrected and ultimately introduce ambiguity into the identification of glomeruli. The inter-individual percentage of unambiguous pairs (51%, Table 5) is significantly smaller than that found in species studied previously with similar quantitative tools, e.g. *B. craniifer* (66%; Rospars and Chambille 1981) and *M. brassicae* (75%; Rospars 1983), as shown by a Wilcoxon rank sum test for equal medians based on the published data. This suggests that the positional variability is higher in *S. littoralis* than in previously investigated species. Whether this is a peculiarity of the species, the strain or a random sampling effect is not known.

Significance of positional variability Our observations are significant for functional studies of ALs because they place

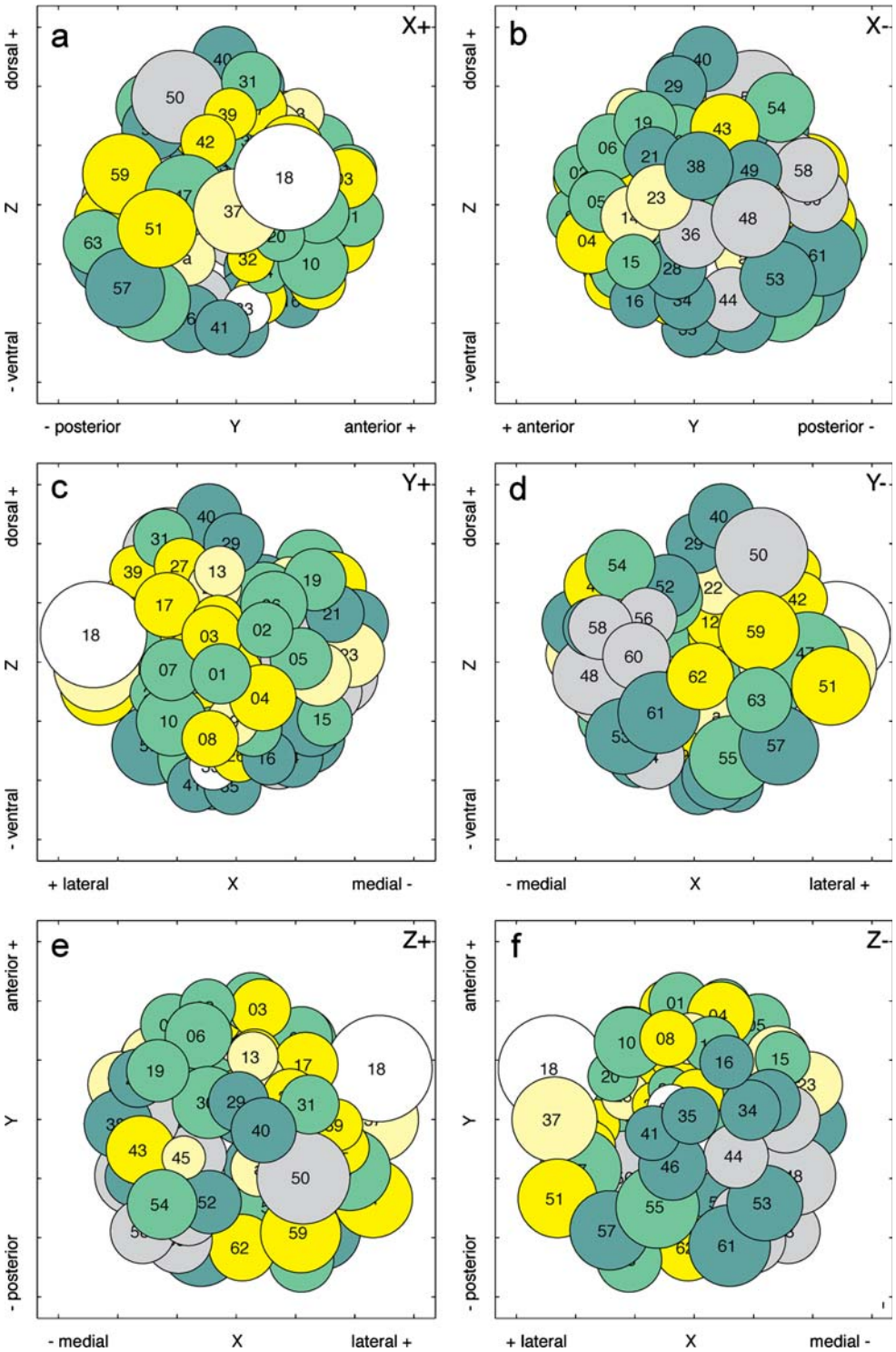

Fig. 7 Computational pairing of the five average ALs shown on the average AL constructed from normalised coordinates of the three ethyl-gallate-stained brains. The AL is shown from six standard viewpoints. **a** Lateral. **b** Medial. **c** Anterior. **d** Posterior. **e** Dorsal. **f** Ventral. The *colour* indicates the number of times each glomerulus was paired by the nearest-neighbour algorithm in ten inter-individual comparisons between the five ALs (*white* 0, *pale yellow* 1 or 2, *yellow* 3 or 4, *light green* 5 or 6, *dark green* 7 or 8, *grey* 9 or 10). Only two glomeruli were never paired: G33 (anomalous) and G18 (the cumulus). The latter example shows that visual and algorithmic pairings are independent and based on different criteria

limits on the possibility of reliably and repeatedly identifying specific glomeruli in a physiological context. For experiments with functional markers, but more importantly when neurons are stained intracellularly from a recording microelectrode (e.g. with neurobiotin), the identification of the glomerulus (or glomeruli) in which the recorded neuron arborises must rely on positional data. This leads to difficulties because the position of a given glomerulus can vary with the global and local distortions of the glomerular array. The availability of a "glomerular map" is then a necessary, but not sufficient, condition for recognising reliably the glomeruli of interest in a given preparation,

Table 6 Effect of normalisation of AL orientation and shape on glomerular pairs[a]

Comp[b]	Norm[c]	Visual pairs			Computational pairs					
		N_v	d_v	Cor_D	App		Id		Dif	
Intra	No[d]	58	41.15±15.85	0.79	29.8	51%	23.4	40%	6.4	10.8%
	Yes[e]	58	22.51±10.52	0.79	40.4	69%	37.0	63%	3.4	5.8%
Inter	No[f]	53.8	67.23±25.17	0.81	27.3	45%	16.6	28%	10.7	17.5%
	Yes[g]	53.8	20.74±10.50	0.81	34.5	57%	31.0	51%	3.5	5.8%

[a] Means of characteristics of visual and computational pairs for five intra-individual comparisons (as in Tables 2, 4) and ten inter-individual comparisons (as in Tables 3, 5). N_v, d_v and Cor_D as in Tables 2, 3. App, Id and Dif as in Tables 4, 5

[b] Intra- or inter-individual comparison (*Comp*)

[c] Glomerular coordinates normalised or not as specified in footnotes d–g below (*Norm*)

[d] No intra-individual normalisation: no sphericisation and no rotation of one AL to restore right-left symmetry

[e] Intra-individual normalisation: sphericisation and rotation of one AL (as in Tables 2, 4).

[f] No intra-individual normalisation but rotation of angle γ around X axis

[g] Intra-individual normalisation and rotation around X, Y and Z axes (as in Tables 3, 5)

because they may be in a slightly different position from that shown on the map. Ideally, knowledge of the coordinates of a glomerulus in a reference coordinate system should be enough to determine its identity. Although this ideal may possibly be reached in some species (a good example is given for the honeybee by Kelber et al. 2006), no evidence exists that such a simple approach can lead to unambiguous identification in glo-

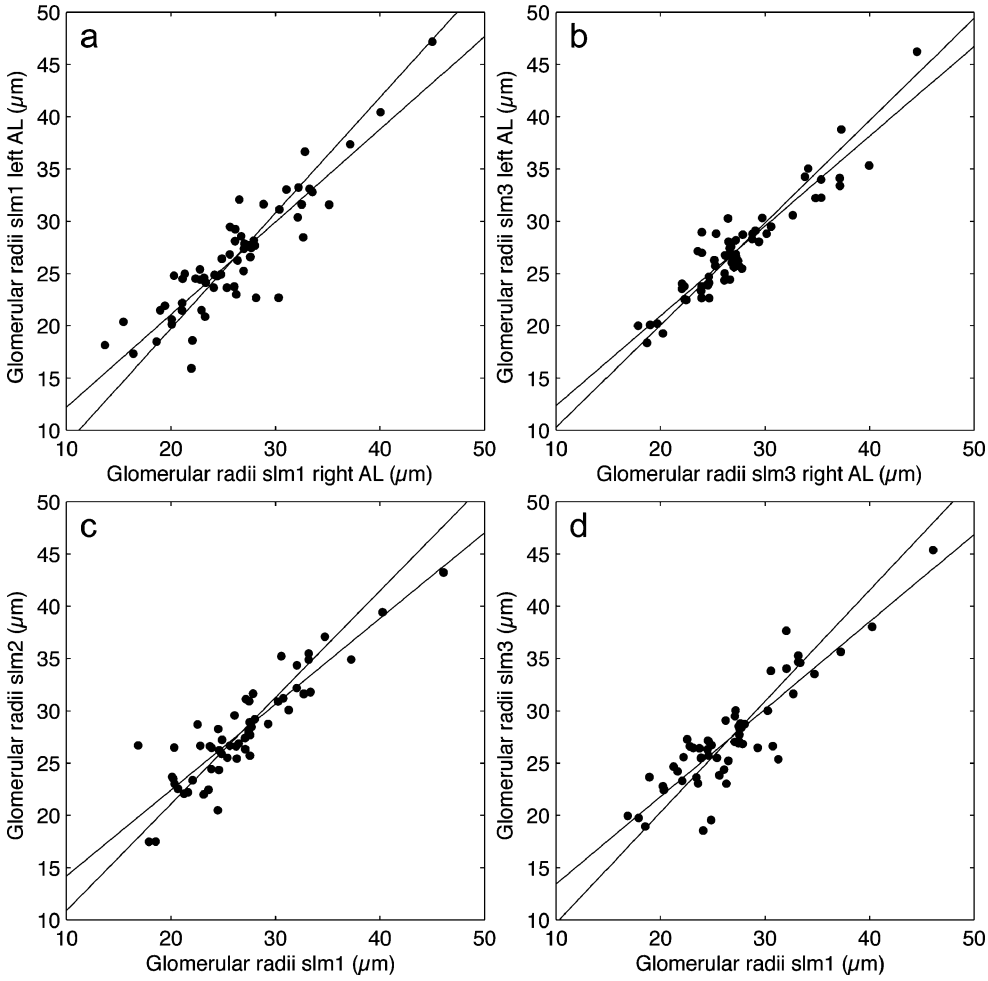

Fig. 8 Example of scatter plots of glomerular sizes. Intra-individual (**a**, **b**) and inter-individual (**c**, **d**) comparisons of visually paired glomeruli. **a** Radius of each right glomerulus of brain slm3 plotted against the radius of its visual homologue in the left AL. **b** Same representation for brain slm1. **c** Mean radius of each right-left pair of brain slm2 plotted against the mean radius of the visually corresponding pair of glomeruli in slm1. **d** Same representation for the brains slm1 and slm3. Regression lines *x/y* and *y/x* are shown. All coefficients of correlation are highly significantly different from zero (Tables 2, 3)

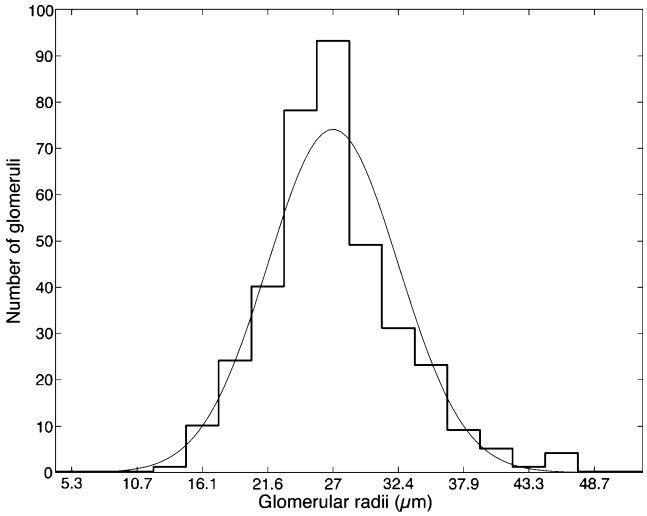

Fig. 9 Distribution of the glomerular radii in ALs of three male *S. littoralis*. Histogram of pooled radii of all 368 glomeruli in right and left ALs of individuals slm1–3 from 14 to 47 μm with a superimposed Gaussian curve of the same mean (27 μm) and standard deviation (5.44 μm) as the sample. Goodness of fit by Kolmogorov-Smirnov test, statistic=0.0772, $P>0.999$

merular arrays of the complexity and variability found, for example, in moths. In a species or strain with small variability, the resulting ambiguities could be resolved by a partial three-dimensional reconstruction of the ALs. With a large variability, comparable to that observed in our *S. littoralis* sample, a more complete reconstruction of the AL may be needed to resolve the ambiguities and to apply normalisation methods.

Number of analysed ALs

To our knowledge, no analysis of ALs with a complete identification of glomeruli has been based on more than ten ALs. For example, the recent study of *Bombyx* ALs by Kazawa et al. (2009) is also based on ten ALs. All other studies of this kind have been based on smaller samples. However, one might still wonder whether ten ALs are enough to quantify the variability of ALs organisation. A common approach for assessing the sensitivity of an estimate to sample size is to examine the extent to which it depends on single data (here ALs). Based on this approach, the variability of parameters describing visually identified glomeruli can be estimated from the data in Tables 2, 3: the intra- and inter-individual correlations between the distances to AL centre and between the sizes are of the order of 0.8, whereas the distances between paired glomeruli are slightly smaller than the mean glomerular radius. Moreover, the range of percentages of agreement between visual and automated inter-individual pairs (about 35%–75%, Table 5) remains stable when discarding any one of the five brains. Thus, no clear indication has been obtained that increasing the sample size will lead to different results.

Concluding remarks

Our data show that different kinds of variance can be distinguished within the AL (apparent versus real; qualitative versus quantitative). These distinctions can be summarised as follows. (1) High apparent glomerular variance does not necessarily mean that AL organisation is disordered. This distinction arises from the observation that several types of apparent distortions of an AL can be corrected by systematic geometrical transforms without identification (scaling) or only partial identification (global rotation, local translations) of glomeruli. The true variance, resulting from random variability, becomes apparent only when these non-random distortions have been corrected. (2) Qualitative invariance, i.e. glomerular identity, does not necessarily imply quantitative invariance. The qualitative invariance of the AL means that each glomerulus has its own characteristics and can, in principle, be individually identified among all others. Quantitative invariance would mean that each glomerulus stays at the same location with the same size. The present results show that, even with a high stability of the number and types of receptor and cerebral neurons and their connections and with correction of the non-random distortions, the location and, to some extent, the size of glomeruli vary considerably. The interplay of developmental processes and mechanical forces might induce the appearance of glomeruli in a location far from their average normalised location as estimated in a sufficiently large sample of brains from the same strain. Moreover, we cannot exclude that significant variations in the number of neurons of different types may also occur. As a result, both the location and size of the same glomerulus (i.e. receiving ORNs expressing the same OR) might significantly vary. In practice, the present results confirm that the production of a glomerular map in a single individual is not sufficient to describe the glomerular array.

The problem of both qualitative and quantitative variability of the glomerular array between individuals has been underestimated so far and is in need of better characterisation. Our study represents a first step towards this goal. It introduces the problem of glomerular variability but further work based on a larger number of ALs and other experimental techniques will be needed to improve our present knowledge. As is becoming increasingly clear, variability is a major problem in neurobiology with obvious consequences for our understanding of connections between neurons in neural networks and reliable information processing despite underlying variations.

Acknowledgments We thank J.-M. Nichols, L. Lloris, C. Chauvet and C. Gaertner for help with insect rearing and technical assistance. R. Barrozo's assistance with the preparation of the figures is greatly acknowledged. We are also grateful to C. Gadenne, N. Varela and D. Jarriault for critically reading an earlier version of the manuscript.

References

Anton S, Hansson BS (1995) Sex pheromone and plant-associated odour processing in antennal lobe interneurons of male *Spodoptera littoralis* (Lepidoptera:Noctuidae). J Comp Physiol [A] 176:773–789

Anton S, Homberg U (1999) Antennal lobe structure. In: Hansson BS (ed) Insect olfaction. Springer, Berlin, pp 98–125

Anton S, Rospars JP (2004) Quantitative analysis of olfactory receptor neuron projections in the antennal lobe of the malaria mosquito, *Anopheles gambiae*. J Comp Neurol 475:315–326

Anton S, Ignell R, Hansson BS (2002) Developmental changes in the structure and function of the central olfactory system in gregarious and solitary desert locusts. Microsc Res Tech 56:281–291

Arnold G, Masson C, Budharugsa S (1985) Comparative study of the antennal lobes and their afferent pathway in the worker bee and the drone (*Apis mellifera*). Cell Tissue Res 242:593–605

Berg BG, Galizia CG, Brandt R, Mustaparta H (2002) Digital atlases of the antennal lobe in two species of tobacco budworm moths, the Oriental *Helicoverpa assulta* (male) and the American *Heliothis virescens* (male and female). J Comp Neurol 446:123–134

Boeckh J, Boeckh V (1979) Threshold and odor specificity of pheromone-sensitive neurons in the deutocerebrum of *Antheraea pernyi* and *A. polyphemus* (Saturnidae). J Comp Physiol 132:235–242

Boissonnat JD, Geiger B (1993) Three dimensional reconstruction of complex shapes based on the Delaunay triangulation. In: Acharya RS, Goldgof DB (eds) Biomedical image processing and biomedical visualization. SPIE, Bellingham, Washington

Bucher D, Scholz M, Stetter M, Obermayer K, Pfluger HJ (2000) Correction methods for three-dimensional reconstructions from confocal images. I. Tissue shrinking and axial scaling. J Neurosci Methods 100:135–143

Carlsson MA, Galizia CG, Hansson BS (2002) Spatial representation of odours in the antennal lobe of the moth *Spodoptera littoralis* (Lepidoptera: Noctuidae). Chem Senses 27:231–244

Chambille I, Masson C, Rospars JP (1980) The deutocerebrum of the cockroach *Blaberus craniifer* Burm. Spatial organization of the sensory glomeruli. J Neurobiol 11:135–157

Couto A, Alenius M, Dickson BJ (2005) Molecular, anatomical, and functional organization of the *Drosophila* olfactory system. Curr Biol 15:1535–1547

Devaud JM, Acebes A, Ramaswami M, Ferrus A (2003) Structural and functional changes in the olfactory pathway of adult *Drosophila* take place at a critical age. J Neurobiol 56:13–23

Distler PG, Boeckh J (1996) Synaptic connection between olfactory receptor cells and uniglomerular projection neurons in the antennal lobe of the American cockroach, *Periplaneta americana*. J Comp Neurol 370:35–46

Distler PG, Boeckh J (1997) Synaptic connections between identified neuron types in the antennal lobe glomeruli of the cockroach, *Periplaneta americana*. I. Uniglomerular projection neurons. J Comp Neurol 378:307–319

Ernst KD, Boeckh J, Boeckh V (1977) A neuroanatomical study on the organization of the central antennal pathways in insects. Cell Tissue Res 176:285–306

Fiala JC (2005) Reconstruct: a free editor for serial section microscopy. J Microsc 218:52–61

Fishilevich E, Vosshall LB (2005) Genetic and functional subdivision of the *Drosophila* antennal lobe. Curr Biol 15:1548–1553

Flanagan D, Mercer AR (1989) An atlas and 3-D reconstruction of the antennal lobes in the worker honey bee, *Apis mellifera* L. (Hymenoptera : Apidae). Int J Insect Morphol Embryol 18:145–159

Galizia CG, McIlwrath SL, Menzel R (1999) A digital three-dimensional atlas of the honeybee antennal lobe based on optical sections acquired by confocal microscopy. Cell Tissue Res 295:383–394

Gao Q, Yuan B, Chess A (2000) Convergent projections of *Drosophila* olfactory neurons to specific glomeruli in the antennal lobe. Nat Neurosci 3:780–785

Ghaninia M, Hansson BS, Ignell R (2007) The antennal lobe of the African malaria mosquito, *Anopheles gambiae*—innervation and three-dimensional reconstruction. Arthropod Struct Dev 36:23–39

Greiner B, Gadenne C, Anton S (2004) Three-dimensional antennal lobe atlas of the male moth, *Agrotis ipsilon*: a tool to study structure-function correlation. J Comp Neurol 475:202–210

Guerenstein PG, Hildebrand JG (2007) Roles and effects of environmental carbon dioxide in insect life. Annu Rev Entomol 53:20–40

Guerenstein PG, Christensen TA, Hildebrand JG (2004) Sensory processing of ambient CO_2 information in the brain of the moth *Manduca sexta*. J Comp Physiol A Neuroethol Sens Neural Behav Physiol 190:707–725

Hallem EA, Dahanukar A, Carlson JR (2006) Insect odor and taste receptors. Annu Rev Entomol 51:113–135

Hansson BS, Anton S (2000) Function and morphology of the antennal lobe: new developments. Annu Rev Entomol 45:203–231

Hansson BS, Christensen TA (1999) Functional characteristics of the antennal lobe. In: Hansson BS (ed) Insect olfaction. Springer, Berlin, pp 125–161

Hanström B (1928) Vergleichende Anatomie des Nervensystems der wirbellosen Tiere. Springer, Berlin

Heisenberg M (2003) Mushroom body memoir: from maps to models. Nat Rev Neurosci 4:266–275

Hildebrand JG, Shepherd GM (1997) Mechanisms of olfactory discrimination: converging evidence for common principles across phyla. Annu Rev Neurosci 20:595–631

Huetteroth W, Schachtner J (2005) Standard three-dimensional glomeruli of the *Manduca sexta* antennal lobe: a tool to study both developmental and adult neuronal plasticity. Cell Tissue Res 319:513–524

Ignell R, Anton S, Hansson BS (2001) The antennal lobe of orthoptera—anatomy and evolution.Brain Behav Evol 57:1-17

Ignell R, Dekker T, Ghaninia M, Hansson BS (2005) Neuronal architecture of the mosquito deutocerebrum. J Comp Neurol 493:207–240

Kanzaki R, Soo K, Seki Y, Wada S (2003) Projections to higher olfactory centers from subdivisions of the antennal lobe macroglomerular complex of the male silkmoth. Chem Senses 28:113–130

Kazawa T, Namiki S, Fukushima R, Terada M, Soo K, Kanzaki R (2009) Constancy and variability of glomerular organization in the antennal lobe of the silkmoth. Cell Tissue Res doi:10.1007/s00441-009-0756-3

Kelber C, Rössler W, Kleineidam CJ (2006) Multiple olfactory receptor neurons and their axonal projections in the antennal lobe of the honeybee *Apis mellifera*. J Comp Neurol 496:395–405

Kent KS, Harrow ID, Quartararo P, Hildebrand JG (1986) An accessory olfactory pathway in Lepidoptera: the labial pit organ

and its central projections in *Manduca sexta* and certain other sphinx moths and silk moths. Cell Tissue Res 245:237–245

Klagges BRE, Heimbeck G, Godenschwege TA, Hofbauer A, Pflugfelder GO, Reifegerste R, Reisch D, Schaupp M, Buchner S, Buchner E (1996) Invertebrate synapsins: a single gene codes for several isoforms in *Drosophila*. J Neurosci 16:3154–3165

Kurylas AE, Rohlfing T, Krofczik S, Jenett A, Homberg U (2008) Standardized atlas of the brain of the desert locust, *Schistocerca gregaria*. Cell Tissue Res 333:125–145

Laissue PP, Reiter C, Hiesinger PR, Halter S, Fischbach KF, Stocker RF (1999) Three-dimensional reconstruction of the antennal lobe in *Drosophila melanogaster*. J Comp Neurol 405:543–552

Leise EM, Mulloney B (1986) The osmium-ethyl gallate procedure is superior to silver impregnations for mapping neuronal pathways. Brain Res 367:265–272

Linster C, Sachse S, Galizia G (2005) Computational modeling suggests that response properties rather than spatial position determine connectivity between olfactory glomeruli. J Neurophysiology 93:3410–3417

Masante-Roca I, Gadenne C, Anton S (2005) Three-dimensional antennal lobe atlas of male and female moths, *Lobesia botrana* (Lepidoptera: Tortricidae) and glomerular representation of plant volatiles in females. J Exp Biol 208:1147–1159

Ochieng SA, Anderson P, Hansson BS (1995) Antennal lobe projection patterns of olfactory receptor neurons involved in sex pheromone detection in *Spodoptera littoralis* (Lepidoptera: Noctuidae). Tissue Cell 27:221–232

Pinto L, Stocker RF, Rodrigues V (1988) Anatomical and neurochemical classification of the antennal glomeruli in *Drosophila melanogaster* Meigen (Diptera: Drosophilidae). Int J Insect Morphol Embryol 17:335–344

Ray A, Goes van Naters W van der, Shiraiwa T, Carlson JR (2007) Mechanisms of odor receptor gene choice in *Drosophila*. Neuron 53:353–369

Rein K, Zöckler M, Mader M, Grübel C, Heisenberg M (2002) The *Drosophila* standard brain. Curr Biol 12:227–231

Reisenman CE, Christensen TA, Hildebrand JG (2005) Chemosensory selectivity of output neurons innervating an identified, sexually isomorphic olfactory glomerulus. J Neurosci 25:8017–8026

Reisenman CE, Heinbockel T, Hildebrand JG (2008) Inhibitory interactions among olfactory glomeruli do not necessarily reflect spatial proximity. J Neurophysiol 100:554–564

Rospars JP (1983) Invariance and sex-specific variations of the glomerular organization in the antennal lobes of a moth, *Mamestra brassicae*, and a butterfly, *Pieris brassicae*. J Comp Neurol 220:80–96

Rospars JP (1988) Structure and development of the insect antennodeutocerebral system. Int J Insect Morphol Embryol 17:243–294

Rospars JP, Chambille I (1981) Deutocerebrum of the cockroach *Blaberus craniifer* Burm. Quantitative study and automated identification of the glomeruli. J Neurobiol 12:221–247

Rospars JP, Chambille I (1986) Postembryonic growth of antennal lobes in the cockroach *Blaberus craniifer*: a morphometric study. Int J Insect Morphol Embryol 15:393–415

Rospars JP, Hildebrand JG (1992) Anatomical identification of glomeruli in the antennal lobes of the male sphinx moth *Manduca sexta*. Cell Tissue Res 270:205–227

Rospars JP, Hildebrand JG (2000) Sexually dimorphic and isomorphic glomeruli in the antennal lobes of the sphinx moth *Manduca sexta*. Chem Senses 25:119–129

Sachse S, Galizia CG (2002) Role of inhibition for temporal and spatial odor representation in olfactory output neurons: a calcium imaging study. J Neurophysiol 87:1106–1117

Sadek MM, Hansson BS, Rospars JP, Anton S (2002) Glomerular representation of plant volatiles and sex pheromone components in the antennal lobe of the female *Spodoptera littoralis*. J Exp Biol 205:1363–1376

Schachtner J, Schmidt M, Homberg U (2005) Organization and evolutionary trends of primary olfactory brain centers in Tetraconata (Crustacea + Hexapoda). Arthropod Struct Dev 34:257–299

Silbering AF, Galizia CG (2007) Processing of odor mixtures in the *Drosophila* antennal lobe reveals both global inhibition and glomerulus-specific interactions. J Neurosci 27:11966–11977

Skiri HT, Ro H, Berg BG, Mustaparta H (2005) Consistent organization of glomeruli in the antennal lobes of related species of heliothine moths. J Comp Neurol 491(4):367–380

Snedecor GW, Cochran WG (1967) Statistical methods, 6th edn. Iowa State University Press, Iowa

Stocker RF, Lienhard MC, Borst A, Fischbach KF (1990) Neuronal architecture of the antennal lobe in *Drosophila melanogaster*. Cell Tissue Res 262:9–34

Strausfeld NJ (1976) Atlas of an insect brain. Springer, Berlin Heidelberg New York

Strausfeld NJ, Hildebrand JG (1999) Olfactory systems: common design, uncommon origins? Curr Opin Neurobiol 9:634–639

Sun XJ, Tolbert LP, Hildebrand JG (1997) Synaptic organization of the uniglomerular projection neurons of the antennal lobe of the moth *Manduca sexta*: a laser scanning confocal and electron microscopic study. J Comp Neurol 379:2–20

Varela N, Couton L, Gemeno C, Avilla J, Rospars JP, Anton S (2009) Three-dimensional antennal lobe atlas of the Oriental fruit moth, Cydia molesta (Busck) (Lepidoptera: Tortricidae): comparison of male and female glomerular organization. Cell Tissue Res (in press)

Vosshall LB, Wong AM, Axel R (2000) An olfactory sensory map in the fly brain. Cell 102:147–159

Wilson RI, Laurent G (2005) Role of GABAergic inhibition in shaping odor-evoked spatiotemporal patterns in the *Drosophila* antennal lobe. J Neurosci 25:9069–9079

Wilson RI, Turner GC, Laurent G (2004) Transformation of olfactory representations in the *Drosophila* antennal lobe. Nature 303:366–370

Zube C, Kleineidam CJ, Kirschner S, Neef J, Roessler W (2008) Organization of the olfactory pathway and odor processing in the antennal lobe of the ant *Camponotus floridanus*. J Comp Neurol 506:425–441